

Article (refereed) - postprint

Salameh, D.; Pey, J.; Bozzetti, C.; El Haddad, I.; Detournay, A.; Sylvestre, A.; Canonaco, F.; Armengaud, A.; Piga, D.; Robin, D.; Prevot, A.S.H.; Jaffrezo, J.-L.; Wortham, H.; Marchand, N. 2018. **Sources of PM_{2.5} at an urban-industrial Mediterranean city, Marseille (France): application of the ME-2 solver to inorganic and organic markers.**

© 2018 Published by Elsevier B.V.

This manuscript version is made available under the CC-BY-NC-ND 4.0 license <http://creativecommons.org/licenses/by-nc-nd/4.0/>



This version available <http://nora.nerc.ac.uk/520790/>

NERC has developed NORA to enable users to access research outputs wholly or partially funded by NERC. Copyright and other rights for material on this site are retained by the rights owners. Users should read the terms and conditions of use of this material at <http://nora.nerc.ac.uk/policies.html#access>

NOTICE: this is the authors' version of a work that was accepted for publication in *Atmospheric Research*. Changes resulting from the publishing process, such as peer review, editing, corrections, structural formatting, and other quality control mechanisms may not be reflected in this document. Changes may have been made to this work since it was submitted for publication. A definitive version was subsequently published in ***Atmospheric Research* (2018), 214, 263-274.**

<https://doi.org/10.1016/j.atmosres.2018.08.005>

www.elsevier.com/

Contact CEH NORA team at
noraceh@ceh.ac.uk

**Sources of PM_{2.5} at an urban-industrial Mediterranean city, Marseille (France):
application of the ME-2 solver to inorganic and organic markers**

**D. Salameh^{1,2*}, J. Pey^{1,4}, C. Bozzetti³, I. El Haddad³, A. Detournay⁵, A. Sylvestre¹, F. Canonaco³,
A. Armengaud⁶, D. Piga⁶, D. Robin⁶, A. S. H. Prevot³, J.-L. Jaffrezo⁷, H. Wortham¹, and N.
Marchand^{1*}**

¹Aix Marseille Univ, CNRS, LCE, Marseille, France.

²French Environment and Energy Management Agency, 20 avenue du Grésillé-BP, 90406 49004 Angers Cedex 01, France

³Laboratory of Atmospheric Chemistry, Paul Scherrer Institute (PSI), 5232 Villigen-PSI, Switzerland

⁴Geological Survey of Spain. Zaragoza IGME Unit, 50006 Zaragoza, Spain

⁵Natural Environment Research Council, Centre for Ecology & Hydrology, Penicuik, UK

⁶AirPACA, Air Quality Observatory in Provence Alpes Côte d'Azur, 13006, Marseille, France

⁷Université Grenoble Alpes, CNRS, IRD, IGE, 38402 St-Martin d'Hères, France

*Corresponding authors:

N. Marchand (nicolas.marchand@univ-amu.fr); D. Salameh (dalia.salameh@univ-grenoble-alpes.fr)

‡Currently at: Université Grenoble Alpes, CNRS, IRD, IGE, 38402 St-Martin d'Hères, France

Abstract

Impacted by a complex mixture of urban, industrial, shipping and also natural emissions, Marseille, the second most populated city in France, represents a very interesting case study for the apportionment of $PM_{2.5}$ sources in a Mediterranean urban environment. In this study, daily $PM_{2.5}$ samples were collected over a one-year period (2011-2012) at an urban background site, and were comprehensively analyzed for the determination of organic carbon (OC), elemental carbon (EC), major ions, trace elements/metals and specific organic markers. A constrained positive matrix factorization (PMF) analysis using the ME-2 (multilinear engine-2) solver was applied to this dataset. PMF results highlighted the presence of two distinct fingerprints for biomass burning (BB1 and BB2). BB1, assigned to open green waste burning peaks in fall (33%; $7.4 \mu\text{g m}^{-3}$) during land clearing periods, is characterized by a higher levoglucosan/OC ratio, while BB2, assigned to residential heating, shows the highest contribution during the cold period in winter (14%; $3.3 \mu\text{g m}^{-3}$) and it is characterized by high proportions from lignin pyrolysis products from the combustion of hardwood. Another interesting feature lies in the separation of two fossil fuel combustion processes (FF1 and FF2): FF1 likely dominated by traffic emissions, while FF2 likely linked with the harbor/industrial activities.

On annual average, the major contributors to $PM_{2.5}$ mass correspond to the ammonium sulfate-rich aerosol (AS-rich, 30%) and to the biomass burning emissions (BB1+BB2, 23%). This study also outlined that during high PM pollution episodes ($PM_{2.5} > 25 \mu\text{g m}^{-3}$), the largest contributing sources to $PM_{2.5}$ were biomass burning (33%) and FF1 (23%). Moreover, 28% of the ambient mass concentration of OC is apportioned by the AS-rich factor, which is representative of an aged secondary aerosol, reflecting thus the importance of the oxidative processes occurring in a Mediterranean environment.

Keywords: Fine particulate matter ($PM_{2.5}$); comprehensive chemical speciation; source apportionment; constrained PMF analysis; biomass burning; fossil fuel combustion; particulate pollution episodes

1. Introduction

Over the last decades, particulate matter with an aerodynamic diameter lower than 2.5 μm ($\text{PM}_{2.5}$) have gained special attention due to its adverse effects on human health. Several studies have demonstrated significant associations between $\text{PM}_{2.5}$ and the increased risk of morbidity and mortality (Dockery, 2009; Laden et al., 2000; Pope and Dockery, 2006). The negative health impact of PM varies regionally, and might be ascribed to heterogeneity in particles, chemical composition and emission sources. As a consequence, a detailed knowledge of the sources of fine PM and a reliable method for the source identification and quantification of their contribution to the ambient levels are urgently needed to support further political reduction strategies.

Various types of source receptor models have been developed and widely used to identify the sources of PM. For a more detailed description of the principles, strengths and weaknesses of these different models the reader can refer to (Belis et al., 2014, 2013; Hopke, 2010; Viana et al., 2008; Watson et al., 2008). In the literature, there is a general paucity of complete and representative chemical profiles of the PM sources, preventing a wide use of CMB (chemical mass balance) model (Watson et al., 1994, 1990). Other multivariate methods such as positive matrix factorization (PMF) have been developed by Paatero and Tapper (1994) and applied to quantitative PM chemical fingerprints, providing both factor profiles and their corresponding temporal contributions. Methodological details of PMF model can be found elsewhere (Paatero, 2004, 1997; Paatero and Tapper, 1994). PMF has been extensively used for PM source apportionment studies. While most of the PMF analysis were carried out on organic carbon/elemental carbon (OC/EC) and inorganic components (i.e. metals/trace elements, and major ions) (Almeida et al., 2015; Bove et al., 2014; Cusack et al., 2013; Hwang and Hopke, 2007, 2006; Mazzei et al., 2008; Minguillón et al., 2012a; Pey et al., 2013a, 2013b; Schembari et al., 2014; Taiwo et al., 2014), very few studies involving organic molecular markers were performed (Callén et al., 2014; Dutton et al., 2010; Heo et al., 2013; Jaeckels et al., 2007; Shrivastava et al., 2007; Zhang et al., 2009), and those combining both inorganic and organic tracers are even more scarce (Bressi et al., 2014; Callén et al., 2009; Minguillón et al., 2012b; Vossler et al., 2016; Waked et al., 2014). However, since the PMF model apportions the sources on the basis of the internal correlations among species, co-linearity induced by processes other than emissions (i.e. seasonal variations, meteorological influences...) often hampers proper separation of the sources. In case of high covariances, the model is typically unable to properly separate two or more factors. This was already pointed out in recent studies (Waked et al., 2014). In order to solve the PMF problem and to optimize the separation of aerosol sources, reasonable and specific constraints based on *a priori* knowledge of the source compositions can be imposed to the factor profiles and/or factor contributions by using the Multilinear Engine-2 (ME-2) solver (Norris and Duvall, 2014; Paatero, 1999). So far, and to the best of our knowledge, the application of the ME-2 solver to offline PM dataset has been only recently used in few studies (Amato et al., 2016; Bozzetti et al., 2017b, 2016; Cesari et al., 2016; Daellenbach et al., 2016; Huang et al., 2014).

In the Marseille urban area, previous studies estimating the OA sources were limited to one intensive field sampling campaign (two weeks in summer 2008), and were performed using two source apportionment techniques, i.e. CMB approach coupled to organic markers and metals, and PMF model applied to AMS (aerosol mass spectrometer) measurements (El Haddad et al., 2013, 2011a, 2011b). The main conclusions highlighted by El Haddad et al. studies were that industrial emissions are associated with ultrafine particles (< 80 nm) and high concentrations of PAH (polycyclic aromatic hydrocarbons) and heavy metals such as Pb, Ni, and V. Both source apportionment techniques (i.e. CMB/markers and PMF/AMS) were in very good agreement and suggested that oxygenated organic aerosol (OOA) constituted the major fraction of the organic aerosol (OA), contributing ~ 80% of OA mass. Further, ^{14}C measurements combined with PMF/AMS data showed that around 80% of such OOA is non-fossil in origin, formed via the oxidation of biogenic precursors, including monoterpenes (El Haddad et al., 2013).

Salameh et al. (2015) highlighted air quality concerns in different Mediterranean cities, with Marseille being one among the five cities involved in that study. Air quality problems in Marseille emerged mainly during the cold season and were attributed to the impact of urban, industrial and biomass burning emissions. In order to discriminate which particular sources are worsening air quality in Marseille and to quantify the influence of each individual source, a PMF source apportionment is performed. The present study aims at investigating the chemical fingerprints of potential $\text{PM}_{2.5}$ sources and their contributions to the ambient PM concentration levels over a one-year period (2011-2012). A constrained PMF analysis was applied to a comprehensive $\text{PM}_{2.5}$ dataset (i.e. inorganic and organic markers) to improve the separation of the key variables (source-specific tracers) among the factor profiles, and thus to generate more representative source profiles and corresponding contributions. This study represents, to the best of our knowledge, a pioneering wide-scale application in southern Europe of a constrained PMF analysis to a comprehensive $\text{PM}_{2.5}$ dataset combining a large number of organic and inorganic chemical species rarely merged together. The methodological knowledge gained from this study highlighted the utility of applying constraints to variables to improve the resolution of the PMF factors, and can provide scientific basis for future source apportionment studies based on offline PM samples.

2. Materials and methods

2.1. Monitoring site and $\text{PM}_{2.5}$ ambient data

A long term monitoring campaign (July 2011-July 2012) was carried out within the framework of EU-MED APICE project (Common Mediterranean strategy and local practical Actions for the mitigation of Port, Industries, and Cities emissions; <http://www.apice-project.eu/>) at an urban background site ("Cinq Avenues": 43°18'18.84"N; 5°23'40.89"E) in Marseille. The objective of the project was to investigate air quality and pinpoint the relative contribution of pollution sources to PM levels in five Mediterranean European cities (e.g. Barcelona, Marseille, Genova, Venice, Thessaloniki), to identify similarities/discrepancies concerning PM characteristics and compositions among these cities (Salameh et al., 2015), and to establish shared strategies to reduce air pollution in port cities.

Marseille, a city with about 1.6 million inhabitants in 2011, ranked as the second most populated city in France. A detailed description of the sampling site and the study area is available in El Haddad et al. (2011b). In brief, Marseille has a large harbor that spans nearly 70 km of the Mediterranean coastline, which is a major hub for the regional and national economy. With a traffic of about 88 million tons of goods handled in 2011, Marseille is also the most important port of the Mediterranean Sea. The city is also in the vicinity of the large petrochemical and industrial complex of Fos-Berre (e.g. petroleum refining, shipbuilding, metallurgical industries) located 40 km northwest of Marseille, and considered among the most important industrial parks in Europe (El Haddad et al., 2011a, 2011b). The region is well-known for its intense photochemical ozone pollution (Flaounas et al., 2009). This active photochemistry, combined with a complex mixture of fugitive PM sources (e.g. urban and industrial emissions) make of Marseille a very interesting and challenging urban-industrial environment for the apportionment of fine aerosol.

Daily PM_{2.5} filter samples were collected onto 150 mm-diameter quartz fiber filters (Tissuquartz) using a high volume sampler (Digitel DA-80) operating at a flow rate of 30 m³ h⁻¹. PM_{2.5} samples were extensively analyzed for the determination of a large number of PM components including organic carbon (OC), elemental carbon (EC), major ions, metals/trace elements and specific organic molecular markers comprising polycyclic aromatic hydrocarbons, *n*-alkanes, hopanes, monosaccharide anhydrides (levoglucosan, mannosan, galactosan), and lignin pyrolysis products (guaiacyl and syringyl derivatives). The analytical methodology as well as the quality control for each chemical species analysis is described in El Haddad et al. (2009), Salameh et al. (2015), and Waked et al. (2014). Moreover, PM_{2.5} mass concentrations were determined using a co-located Tapered Element Oscillating Microbalance equipped with a Filter Dynamic Measurement System (TEOM-FDMS, Thermo Scientific).

2.2. Chemical speciation of PM_{2.5} filter samples

A total of 216 PM_{2.5} filter samples were collected during the measurement campaign, which covers 62% of the period of the study (i.e. 30 July 2011 to 20 July 2012). Some of the samples were merged together and analyzed as composite samples based on the temporal variation of the concentrations of PM₁₀, PM_{2.5}, or gaseous pollutants (e.g. SO₂). Samples collected during high PM pollution events (e.g. daily PM_{2.5} concentration above the WHO daily limit of 25 µg m⁻³; (WHO, 2006)), or with any other specific pollution episodes (e.g. SO₂) were analyzed individually (i.e. 24h samples) (Fig A-1, Appendix A, supplementary material). Finally, the chemical speciation of PM_{2.5} samples (except the OC and EC analysis) was performed on a total of 55 samples (i.e. 45 composite and 10 individual samples), using a range of instrumental techniques which are presented briefly as follows:

- **Organic and elemental carbon** (OC and EC) concentrations were determined using a 1.5 cm² punch of each individual filter by a Thermal Optical Transmittance (TOT) technique using a Sunset Laboratory Analyzer Instrument (Birch and Cary, 1996; Jaffrezo et al., 2005), following EUSAAR2 protocol (Cavalli et al., 2010).

- **Major ionic species** (SO₄²⁻, NO₃⁻, Cl⁻, NH₄⁺, K⁺, Na⁺, Mg²⁺, and Ca²⁺) were analyzed by ionic chromatography (IC), after extraction of a fraction of the samples in ultra-pure water. The description of the method has been presented in detail by Jaffrezo et al. (1998).

- **Metals and trace elements** (6 major elements Al, Ca, Fe, K, Mg, Na, as well as 27 other trace elements, e.g. As, Ba, Cd, Ce, Co, Cr, Cs, Cu, La, ..., Ni, V, Zn, Zr) were analyzed by Inductively Coupled Plasma Mass Spectrometry (ICP/MS), after an acidic digestion of a fraction of the samples using a mixture of inorganic acids (HNO₃:HF) (Waked et al., 2014).

- **Speciated organic compounds**, including monosaccharides anhydrides (levoglucosan, mannosan, galactosan), lignin pyrolysis products (guaiacyl and syringyl derivatives), *n*-alkanes, hopanes, and polycyclic aromatic hydrocarbons (PAH) were quantified using a Trace GC 2000 chromatograph coupled to an ion trap mass spectrometer following the analytical methodology described in detail in El Haddad et al. (2011a, 2009).

Field blank filters were also collected and analyzed following the same analytical procedures described above. All the quantified species were blank corrected (see Appendix A).

Details on the used method to obtain the PM_{2.5} chemical mass closure were reported in Salameh et al. (2015). Concisely, organic matter (OM) concentrations were obtained by applying a factor of 1.4 to the OC concentrations (Putaud et al., 2010). The non-sea salt sulfate (nss-SO₄²⁻) concentrations were calculated by subtracting the sea salt sulfate (ss-SO₄²⁻; where ss-SO₄²⁻ = 0.252 × Na⁺) from the total mass concentration of sulfate (Seinfeld and Pandis, 1998). The sea salt concentrations were calculated from soluble sodium concentrations (3.252 × Na⁺; (Grythe et al., 2014)). Mineral matter concentrations were estimated from the sum of Al₂O₃, SiO₂, CO₃²⁻, Ca, Fe, K, Mg, Mn, and Ti, where Al₂O₃, SiO₂, CO₃²⁻ were indirectly determined using empirical equations (Pérez et al., 2008). The seasonal variation of the PM_{2.5} concentrations is described in detail in Salameh et al. (2015) and a brief overview of the main organic and inorganic markers concentrations and seasonal evolutions is provided in the supplementary material (Appendix A).

2.3. Source apportionment of PM_{2.5}: ME-2 solver

PMF (Paatero and Tapper, 1994) is a bilinear statistical model using a weighted least-squares algorithm to describe the variability of an input data matrix (**X**) as the product of a factor profile matrix (**F**) and a factor contribution matrix (**G**) (Paatero, 1997; Paatero et al., 2005; Paatero and Hopke, 2003) as according to the following equation:

$$\mathbf{X} = \mathbf{G} \mathbf{F} + \mathbf{E}$$

Where **E** is the residual matrix, i.e. the difference between the measurement X and the product of the modelled G and F matrices.

PMF imposes non-negative constraints on G and F, and finds the solution that minimizes the objective function Q, defined as the sum of the squared residuals (*e_{ij}*) weighted by their respective uncertainties (*σ_{ij}*):

$$Q = \sum_{i=1}^m \sum_{j=1}^n \left(\frac{e_{ij}}{\sigma_{ij}} \right)^2$$

Canonaco et al. (2013) reported that the monitoring of the total Q is not meaningful because the expected value (Q_{expected}) depends on the size of the data matrix and on the number of chosen factors, and suggested to investigate the relative change in the Q/Q_{expected} ratio across different models runs.

PMF algorithm may have a substantial degree of rotational ambiguity specific to factor analytic models, meaning that multiple solutions (**G**, **F**) can be associated with the same Q value (see Paatero et al. (2002) for more details). To direct the solution toward environmentally meaningful rotations the PMF algorithm was solved using the “*a* value” approach of the ME-2 solver (Paatero, 1999), implemented in the Source Finder (SoFi) toolkit (SoFi v4.8, <http://psi.ch/HGdP>, Canonaco et al., 2013), within the Igor Pro software package (Wavemetrics Inc., Lake Oswego, Oregon, USA) and following the good practices of the “European guide on air pollution source apportionment with receptor models” (Belis et al., 2014) (Appendix B, for more details). Different approaches can be exploited with the ME-2 solver and are discussed in detail elsewhere (Canonaco et al., 2013; Norris et al., 2009; Paatero and Hopke, 2009). Briefly, the “*a* value” technique used in this study allowed an efficient exploration of the solution space *by a priori* constraining individual elements of the factor profiles within a certain variability defined by the scalar *a* ($0 \leq a \leq 1$) (Canonaco et al., 2013). The methodological procedure implemented and applied here comprised two steps. Firstly, different number of factors (*p*) were examined to retrieve the reasonable solution that represents the best fit of the dataset (**Sect. 2.3.2; Fig B-1**, Appendix B, supplementary material). Afterward, a relevant set of chemical constraints defined based on *a priori* knowledge of the source compositions was imposed to a subset of species in the PMF factor profiles (*a* value set to zero). A complete discussion of the constraints applied within the framework of the “*a*-value” approach is presented in **Sect. 2.3.2**.

2.3.1. Data analysis: PMF inputs

PMF analysis requires as input the measured concentrations of chemical species and the corresponding uncertainties. The selection of input species was based on the percentage of values above the detection limit (DL), and the signal-to-noise (S/N) ratio for each species (Paatero and Hopke, 2003), with a special focus on highly specific organic and inorganic source markers (e.g. biomass burning, traffic, other combustion sources). The uncertainties were determined following the methodology described by Gianini et al. (2012) and recently applied by Waked et al. (2014). It uses DL (twice of the standard deviation of the blanks), the coefficient of variation (CV calculated as the standard deviation of repeated analyses divided by the mean value), and an additional factor (*a* of 0.03) to account for additional sources of uncertainty. In the input data matrix of the unconstrained PMF analysis, concentrations below DL were replaced by DL/2 with uncertainties estimated as 5/6 of the DL value, and species with 60% of the values below detection limit (BDL) were excluded. According to the S/N criterion (Paatero and Hopke, 2003), “weak” variables (S/N between 0.2 and 2.0) were downweighted by increasing their uncertainties by a factor of 3 (Paatero and Hopke, 2003), while “bad” variables (S/N < 0.2) were excluded. The final input dataset retained for further PMF analysis (i.e. constrained PMF) is displayed in **Table 1**. It includes 37 chemical species categorized as “strong” variables (S/N > 2) and highly source specific, i.e. 25 organic markers (OC, EC, 3 PAH, 10 *n*-alkanes, 3 hopanes, 2 monosaccharide anhydrides, and 5 methoxyphenols) and 12 inorganic markers (6 major ions, 6 trace elements/metals) (**Table 1**). The seasonal variability in the concentrations of these markers is described in detail in the supplementary material (**Fig A-2**, appendix A). The data statistics (i.e. arithmetic mean, median, minimum, maximum, BDL, S/N ratio) of the input species and the

correlation matrix are reported in **Table B-1a** and **1b**, respectively. It is noteworthy that double counting of pairs of elemental and ionic species (e.g. Na^+ and Na, K^+ and K, Ca^{2+} and Ca) is avoided by including the ionic soluble concentration for sodium and potassium (i.e. Na^+ , K^+), and the total concentration obtained by ICP-MS for calcium (with no values below DL). Owing to the fact that some organic molecular markers (e.g. levoglucosan, mannosan, etc.) are used in the model, the OC was replaced by OC^* , defined as: $[\text{OC}^*] = [\text{OC}] - (0.95 \times [\text{PAH}] + 0.85 \times [n\text{-alkanes}] + 0.87 \times [\text{hopanes}] + 0.44 \times [\text{levoglucosan}] + 0.44 \times [\text{mannosan}] + 0.59 \times [\text{syringaldehyde}] + 0.57 \times [\text{vanillic acid}] + 0.65 \times [\text{acetovanillone}] + 0.63 \times [\text{syringylacetone}] + 0.55 \times [\text{syringic acid}])$ in order to prevent double counting of carbon species. These coefficients were determined based on the carbon content of each organic compound (Waked et al., 2014). To obtain the source contributions to the total measured PM mass, the usual multilinear regression analysis of the measured PM mass against the estimated source contributions was applied (Pey et al., 2013b).

Table 1 : Outline of the characteristics of PM dataset used in PMF analysis

Site	"Cinq avenues", Marseille (France)
Time period	30 July 2011 – 20 July 2012
PM sampling	24 h $\text{PM}_{2.5}$ samples (216 filters)
Number of chemical species	37
Carbonaceous species	OC^* and EC
Ionic species	Cl, NO_3^- , SO_4^{2-} , Na^+ , NH_4^+ , K^+
Metals/trace elements	Ca, Cu, Fe, Ni, Pb, V
Organic markers	benzo[a]anthracene, benzo[a]pyrene, benzo[ghi]perylene;
	n-C20, n-C21, n-C22, n-C23, n-C24, n-C25, n-C26, n-C28, n-C29, n-C31;
	17 α (H)-21 β (H)-norhopane, 17 α (H)-21 β (H)-hopane, 17 α (H)-21 β (H)-22S-homohopane;
	levoglucosan, mannosan, syringaldehyde, vanillic acid, acetovanillone, syringyl acetone, syringic acid

2.3.2. Number of factors and set of constraints

When applying PMF, the determination of the number of factors is the most critical step. We select the number of factors providing the best description of the dataset, here defined as an environmentally interpretable representation of the data. This selection is always a compromise: not enough factors may lead to poorly separated sources, whereas too many factors may lead to a mathematical split of the factors, which is not necessarily environmentally relevant. Here, we have examined solutions from 2 to 12 factors in the unconstrained PMF runs, each of which initialized from 20 different random starting points.

The determination of the optimal number of factors was performed after evaluating a number of criteria including: (a) the variation of Q/Q_{expected} ratio from 2 to 12 factors (**Fig. B-1a**) (Canonaco et al., 2013; Polissar et al., 2001); (b) the scaled residuals with the variation of IM (maximum individual column mean) and IS (maximum individual column standard deviation) as a function of the number of factors (**Fig. B-1b**) (Lee et al., 1999); and (c) the reasonable geochemical likeliness of factors chemical composition and factors time-series. The Q/Q_{expected} ratio decreased continuously from 3.8 to 0.7 when the number of factors increases from 2 to 12 factors (**Fig. B-1a**). Small changes in the Q/Q_{expected} ratio were observed for solutions between 7 and 10-factors suggesting a little improvement with extra factors. The IM and IS values decreased with the number of factors and become more

steady for solutions starting from 5 factors (**Fig. B-1b**). Therefore, solutions from 5 to 10 factors were carefully examined. Based on the key criterion of extracting realistic and reasonable source profiles and contributions and on the evaluation of the aforementioned parameters ($Q/Q_{expected}$, IM, and IS), a 7-factor solution ($Q/Q_{expected}$ of 1.43, unexplained variation of all input variables < 25%) was selected as the most reasonable solution for this dataset (**Fig. B-1**). Rotational ambiguity (Paatero et al., 2002) was explored by varying the Fpeak parameter between -1 and 1, with steps of 0.1. Solutions for Fpeak values outside this range showed factors with no physical meaning or that did not converge. Since the rotated solutions did not appear to improve the source profiles, the non-rotated solution (Fpeak=0) was chosen. The seven factors resolved by unconstrained PMF analysis were identified as follows: biomass burning (described by two factors BB1 and BB2); road traffic; fossil fuel combustion (described by two factors FF1 likely related to traffic emissions and FF2 to harbor activities/ships emissions); ammonium sulfate rich; and the last factor is a mixed factor of multiple primary emission sources (e.g. sea salt, traffic, and vascular plant waxes) possibly related to wind resuspension. The seven unconstrained PMF factor profiles expressed each one as the percentage of the total mass in the factor of each 37 chemical species are reported **Table B-2**. The unconstrained PMF results showed a certain degree of mixing between the factors, where some specific source tracers were not properly distributed into the factors they should belong to. This may be related to the relatively limited number of samples used in PMF analysis (i.e. 55) which might reduce the resolving power shown by PMF and the interpretation of the results should be made cautiously. For example, the biomass burning factor explained up to 29% of the hopanes mass concentration, specific markers of vehicular emissions, whereas 12% of acetovanillone mass concentration is explained by FF1. It should be noted that mixing issues are inherent to the PMF approach based on the internal correlation within the data set and where solutions are subject to rotational ambiguity, which complicates the interpretation of the profiles. PMF algorithm extracts static factor profiles, which implicates a constant chemical composition over the monitoring period. Nevertheless, the variability of the concentration of a given species depends on a number of parameters such as the source emission strengths or the meteorological conditions (e.g. temperature, pressure, boundary layer height, rainfall, etc.). The variation of source profiles with time is further accentuated by the use of species with different physicochemical properties, where the combination of non-volatile and non-reactive species (trace elements/metals, EC) with semi-volatile and slightly reactive species (organic markers) can induce distortion of the chemical fingerprint of the different resolved factors and potentially lead to the appearance of "atypical factors".

In order to improve the factor separation and to handle the problem of rotational ambiguity, a constrained PMF analysis using the "a value" approach of the ME-2 solver was performed (Canonaco et al., 2013). A set of physically meaningful constraints from well-characterized sources defined based on *a priori* knowledge of the source fingerprints was applied to a subset of species in the PMF factor profiles (**Table B-3**). In brief, the contributions of some species have been fully constrained (a value=0) in the factor fingerprints, as follows:

(a) Contributions of anhydrous sugars and methoxyphenols, specific tracers of biomass burning emissions (Simoneit et al., 1999), were set to zero in all profiles, except the biomass burning (BB) factors (**Table B-3**);

(b) Contributions of hopanes, markers of fossil fuel combustion (El Haddad et al., 2009), were only authorized in factors related to road traffic and fossil fuel combustion, imposing their contributions to zero in all other factors;

(c) Contributions of vanadium and nickel, typical tracers of heavy oil combustion (Viana et al., 2009), have been constrained to zero in all profiles, except the FF2 (**Table B-3**). We note that the crustal enrichments factors (EFs) of V and Ni were evaluated using Al as a reference element and the upper crust composition reported in Hans Wedepohl (1995). EFs values of both elements were around ~50, which indicates that V and Ni are significantly enriched, and are probably more attributed to non-crustal, anthropogenic sources.

2.3.3. Quality and robustness of constrained PMF results

With these constraints applied to the initial PMF results, the residuals scaled by the uncertainty resulting from the constrained PMF analysis were almost normally distributed for most species, and were within the range of ± 4 (**Fig. B-2b**). The ratio between PMF-reconstructed and measured concentrations for the input variables shows generally values close to one except for syringaldehyde and acetovanillone (**Fig. B-2a**). Further, good correlations were observed between the measured and reconstructed concentrations for $PM_{2.5}$ (**Fig. B-2c**) and for most of the input species, showing a good coefficient of determination ($R^2 > 0.8$), except Na^+ , Ni and syringaldehyde which were less well modeled ($R^2 = 0.6$) (**Table B-4**), probably due to the fact that PMF model is not always able to accurately model species having low concentrations and high uncertainties (Waked et al., 2014).

3. Results and discussions

3.1. Factor profiles: source identification

The seven factors resulting from the constrained PMF analysis were identified based on the characteristics chemical species (i.e. specific source tracers) in the factor fingerprints (**Fig. 1**), with high percentage of their ambient concentration apportioned by a factor (**Fig. B-3**). The identified $PM_{2.5}$ factors are related to (a) biomass burning (two factors), (b) fossil fuel combustion (two factors), (c) road dust, (d) ammonium sulfate (AS) rich and (e) aged sea salt/dust rich. It should be noted that compared to the unconstrained PMF analysis, the constrained solution showed a more proper distribution of the specific source tracers with an improvement in the factor separation. For instance, an aged sea salt/dust rich was identified in the constrained PMF solution, while it was mixed with a traffic contribution in the unconstrained analysis. The factor profiles (in $\mu g \mu g^{-1}$ of $PM_{2.5}$) were presented in **Figure 1** and were also reported in **Table B-5** and will be discussed in detail in the following subsections.

- **Factor 1 – Biomass burning 1 (BB1)**

Factor 1 was identified to be related to biomass burning (BB1), based on the high percentage of the ambient concentrations of monosaccharide anhydrides (e.g. mannosan (89%), levoglucosan (67%)), and methoxyphenols (acetovanillone (73%), and syringyl acetone (58%)) apportioned by this factor (**Fig. 1**).

A relatively high percentage of NH_4^+ , K^+ , NO_3^- , Cl^- , OC, and EC was also observed (28%, 25%, 24%, 22%, 17%, and 8%, of their ambient concentration, respectively). Fine potassium is often used as an indicator of biomass burning in many source apportionment studies (Puxbaum et al., 2007; Reche et al., 2012). It is important to mention that 24% of the ambient nitrate concentration is apportioned by BB1 and the model was unable to resolve a nitrate-rich factor from the analyzed dataset, which is probably due to the presence of strong collinearities between the nitrate-rich and BB factors (i.e. similar seasonal patterns). This might induce a bias in the analysis, and most probably leads to a possible overestimation of the impact of biomass burning emissions. In this study, NO_3^- contributed to 8.7% of the BB1 mass (**Table B-5**), which is still environmentally realistic considering NO_x emissions from biomass burning. Further, the current state of knowledge on the chemical profiles of BB and nitrate-rich factors does not allow proper forcing for their appropriate separation (i.e. constraining NO_3 in BB).

Interestingly, a significant percentage of the ambient concentration of *n*-alkanes with an odd carbon number was apportioned by BB1, i.e. *n*-C29 (28%), and *n*-C31 (21%) (**Fig. 1** and **Fig. B-3**). As mentioned previously, high molecular weight *n*-alkanes are derived from epicuticular waxes of higher plants, and are emitted in significant proportions during the growing season (e.g. intense solar radiation and high surface temperature) (Graham et al., 2003; Simoneit et al., 1991). However, significant amounts of *n*-C29 and *n*-C31 concomitant with higher concentrations of levoglucosan are observed during fall (**Fig. A-2**), period in which the living biomass is generally considered as dormant. BB1 showed an important contribution during late fall (land clearing periods) with a maximum of $24.4 \mu\text{g m}^{-3}$ (11/26/2011; **Fig. 1**), and is characterized by a higher levoglucosan/OC ratio, probably resulting from the open green waste burning, a practice that is widespread in Marseille surrounding areas during this season, and emits large amounts of epicuticular plant waxes (Hays et al., 2002). In addition, we note that the average daily temperature prevailing between the end of October and early November is around 17°C (maximum of 20°C , Marignane station) with a BB1 contribution up to $5 \mu\text{g m}^{-3}$ (i.e. 27% of $\text{PM}_{2.5}$). The higher temperatures observed during that period compared to winter season (average temperature of 6°C with a minimum of -4°C), is also supporting the hypothesis of the potential influence of emissions from open green waste burning, rather than residential heating.

- **Factor 2 – Biomass burning 2 (BB2)**

As for factor BB1, a high percentage of the ambient concentration of lignin pyrolysis products and monosaccharide anhydrides was apportioned by BB2, e.g. syringyl acetone (95% of the ambient concentration), vanillic acid (88%), syringaldehyde (81%), and levoglucosan (33%), and was therefore also assigned to biomass burning (BB2) (**Fig. 1**). As already observed for BB1, 21% of the ambient nitrate concentration was apportioned by BB2, and the same explanation drawn up for BB1 is also suggested for BB2. Compared to BB1, a high percentage of the ambient concentration of PAH (47-63%), and *n*-alkanes (< *n*-C24; 18-36%) was apportioned by this factor, which is probably related to

the cold and stable atmospheric conditions favoring the transfer of semi-volatile organic species to the particulate phase. This assumption is corroborated by the examination of the temporal variation of BB2 (**Fig. 1**), which exhibited a maximum contribution of $13 \mu\text{g m}^{-3}$ during the coldest period of the year (02/10 to 02/13/2012; temperature between -3.5 and -0.7 °C). Compared to BB1, BB2 is characterized by high proportions from lignin pyrolysis products from the combustion of hardwood, with maximum contributions during the coldest period of winter (January, February), and is likely to be more related to residential heating (**Fig. 1** and **Fig. B-3**).

It should be noted that even when decreasing the number of factors from seven to six in the unconstrained PMF runs, the two biomass burning signatures are still separated. This highlights the robustness of the separation of the two factors and suggests that they do represent two different burning processes: residential heating versus open green waste burning. While BB2 shows maximum contributions during the cold period in winter with a high contribution from lignin pyrolysis products from the combustion of hardwood, BB1 presents high contributions in late fall during land clearing periods probably resulting from the combustion of cellulose rich biomass. It is important to emphasize that this study represents to the best of our knowledge, one of the first identification of an open green waste burning signature and its separation from domestic heating. Moreover, offline-AMS source apportionment results performed on PM filters collected at the same study period in Marseille also revealed an evolution in the biomass burning composition (Bozzetti et al., 2017a).

- **Factor 3 – Fossil fuel combustion 1 (FF1)**

Factor 3 explained high percentage of the ambient concentration of hopanes (45-61%), lower molecular weight *n*-alkanes ($< n\text{-C}_{28}$; 35-59%), PAH (26-31%), OC* (28%), Pb (24%), and EC (16%). This factor seems to be likely dominated by traffic emissions mixed with a non-traffic fossil combustion source (e.g. industrial processes) and was therefore assigned to FF1 (El Haddad et al., 2009; Waked et al., 2014). It is worth noting that OC* was the dominant component of this factor, accounting for 73% of PM_{2.5} mass attributed to this factor. The average OC/EC ratio in this source profile was 6.25, which points out to a strong OC enrichment compared to EC. The temporal evolution of FF1 displayed a specific and clear seasonal behavior and showed a substantial increase of the concentrations during the cold period with a maximum up to $18 \mu\text{g m}^{-3}$ (01/09/2012), and relatively homogeneous concentrations for the rest of the year (**Fig. 1**). Such winter enhancement is likely to be the upshot of the combination of two main factors: (i) the condensation of semi-volatile organic compounds favored by low temperature encountered during this period (6 °C on average with a minimum of -4 °C); and (ii) the higher atmospheric stability and lower mixing-layer height favoring the confinement of pollutants within the emission area, typical in winter. This atypical signature reflects the particular behavior of the semi-volatile organic markers and highlights the semi-volatile character of this factor. It should be recalled that PMF algorithm extracts static factor profiles, and in our study the combination of non-reactive species (e.g. trace elements) with semi-volatile and slightly reactive species (organic markers) can induce distortion in the matrix resolution leading potentially to the appearance of “atypical factors” (**Sect. 2.3.2**).

- **Factor 4 – Road dust**

As shown in **Figure 1**, the factor 4 is characterized by a high percentage from the road dust components, i.e. Cu (71% of the ambient concentration), Fe (32%), and Ca (25%), which are typical in urban environments, and was thus identified as the resuspension of road dust. Ca and Fe are typical mineral constituents and can be re-suspended by road traffic, while Cu is known to be emitted from brake wear, tire wear and road wear (Karanasiou et al., 2009; Schauer et al., 2006; Sternbeck et al., 2002). The presence of Ca in this profile could also be related to the intense construction activities conducted in Marseille during the period under consideration. The temporal evolution of this factor showed the highest concentrations in fall and summer, reaching up to $9 \mu\text{g m}^{-3}$ and $4 \mu\text{g m}^{-3}$, respectively (**Fig. 1**) and corresponding to the driest periods.

- **Factor 5 – Fossil fuel combustion 2 (FF2)**

The ambient concentrations of V and Ni, typical tracers of heavy fuel oil combustion, were only apportioned by factor 5, because their mass fraction was subsequently forced to 100% in this factor (**Sect. 2.3.2**). V and Ni sources may be industrial processes (e.g. oil refineries, power plants, boilers, etc.), and ship emissions (Mooibroek et al., 2011; Moreno et al., 2010). Due to similar fuel and combustion conditions, it may be difficult to distinguish between these two sources (Viana et al., 2014, 2009), therefore, this factor was identified as the contribution from FF2. However, the evaluation of V/Ni ratio suggest larger contributions from ship emissions (Moreno et al., 2010; Pandolfi et al., 2011). The source profile is characterized by an average V/Ni ratio of 2.35, which is in agreement with the characteristic ratios for ship emissions (ranging from 2.5 to 3.5) (Agrawal et al., 2008; Bove et al., 2014; Pandolfi et al., 2011; Viana et al., 2014), reflecting the large impact of the harbor activities and the significant influence from vessel emissions. A high variance of hopanes (39-55% of the ambient concentration) was explained by this factor and could possibly originate from coal and coke emissions (Oros and Simoneit, 2000; Weitkamp et al., 2005; Zhang et al., 2008). This factor also explains a noticeable variance of sulfate (22% of the ambient sulfate concentration), and other species such as EC (32%), Ca (17%), Fe (16%), Pb (13%), *n*-alkanes (3-16%), PAH (4%). It should be noted that EC was a dominant chemical component of this factor, accounting for 36% of $\text{PM}_{2.5}$ mass attributed to this factor. The OC/EC ratio in this factor is 0.17 (Table B-5), comparable to that reported recently by Amato et al. (2016) at an urban background site in Barcelona (OC/EC of 0.22 in heavy oil combustion factor). The high proportions of EC and hopanes in this factor could be also linked to the heavy-duty trucks traffic in the industrial/harbor area of Fos-Berre (Sylvestre et al., 2017). As depicted in **Figure 1**, the temporal trend of this factor showed highest concentrations during warm periods reaching up to $13.7 \mu\text{g m}^{-3}$ (07/19/2012). These observations are expected and were consistent with summer wind patterns and the industrial vicinity of Marseille among which the Fos-Berre area located northwest the city (El Haddad et al., 2011a), where there is a high density of industries and strong emissions from maritime transport sector. In fact, during summertime, and in low Mistral ($< 3 \text{ m.s}^{-1}$) conditions, sea breeze circulation prevails and is often associated with high pollution levels over Marseille due to the low dispersion of pollutants. In the early morning of such days, Marseille is directly downwind of the industrial area and, as the temperature of the surface of the land rises, sea breeze wind speed

increases. It results in an increased residence time of the industrial polluted air masses over the Mediterranean Sea before they arrive over Marseille (El Haddad et al., 2011a).

- **Factor 6 – Ammonium sulfate rich**

The factor 6 was assigned to ammonium sulfate (AS)-rich due to the presence of high percentage of ammonium and sulfate (42% and 56% of their ambient concentration, respectively) apportioned by this factor (**Fig. 1**). The average concentration ratio between SO_4^{2-} and NH_4^+ in the factor is 2.85, which is consistent with the stoichiometric ratio for ammonium sulfate (i.e. 2.66 by mass). This means that the SO_4^{2-} is mainly in the form of $(\text{NH}_4)_2\text{SO}_4$. This factor contains an important contribution from OC (31%), which is probably due to the formation of secondary OC via gas-to-particle conversion. The presence of a significant proportion of OC in a AS-rich factor was also observed in PMF studies at other sites (Amato et al., 2016; Bozzetti et al., 2017b; Cesari et al., 2016; Waked et al., 2014), and can be explained by the similarities in the chemical processes leading to the formation of ammonium sulfate and secondary organic aerosol (SOA) (Waked et al., 2014). The temporal evolution of the AS-rich shows rather homogeneous contributions throughout the year (**Fig. 1**), highlighting the regular impact of aged background aerosol.

- **Factor 7 – Aged sea salt/dust rich**

Factor 7 is a mixed source of aged sea salt and dust resuspension, since a high percentage of the ambient Na^+ concentration (55%), a typical tracer for sea salt is apportioned by this factor (**Fig. 1**). The $\text{Cl}^- : \text{Na}^+$ mass ratio in this factor was equal to 0.37, which is much lower than the bulk sea water mass concentration ratio (1.8) (Seinfeld and Pandis, 1998). The excess of Na^+ in this factor can be the result of the reaction of NaCl with acidic species, such as H_2SO_4 and HNO_3 leading to a displacement of Cl^- as HCl and the formation of NaNO_3 or Na_2SO_4 (Hwang and Hopke, 2007; Pio et al., 1996). The high percentage of Ca and Fe apportioned by this factor (58% and 36% of their ambient concentration, respectively) could be related to the combined effect of dust emitted from renovation and construction activities in the harbor area and all over the city together with sea-breeze development carrying sea salt particles inland. Nevertheless, Ca and Fe have been recently identified as highly emitted by steel plant activities and specifically by the main steel plant located in the Fos/Berre industrial area (Sylvestre et al., 2017). Therefore, an industrial influence to this factor cannot be excluded. A high percentage of the ambient concentration of *n*-alkanes with an odd carbon number is also apportioned by this factor, i.e. *n*-C29 (69%) and *n*-C31 (77%), and is related to the wind-blown resuspension of seasalt, dust, and plant waxes.

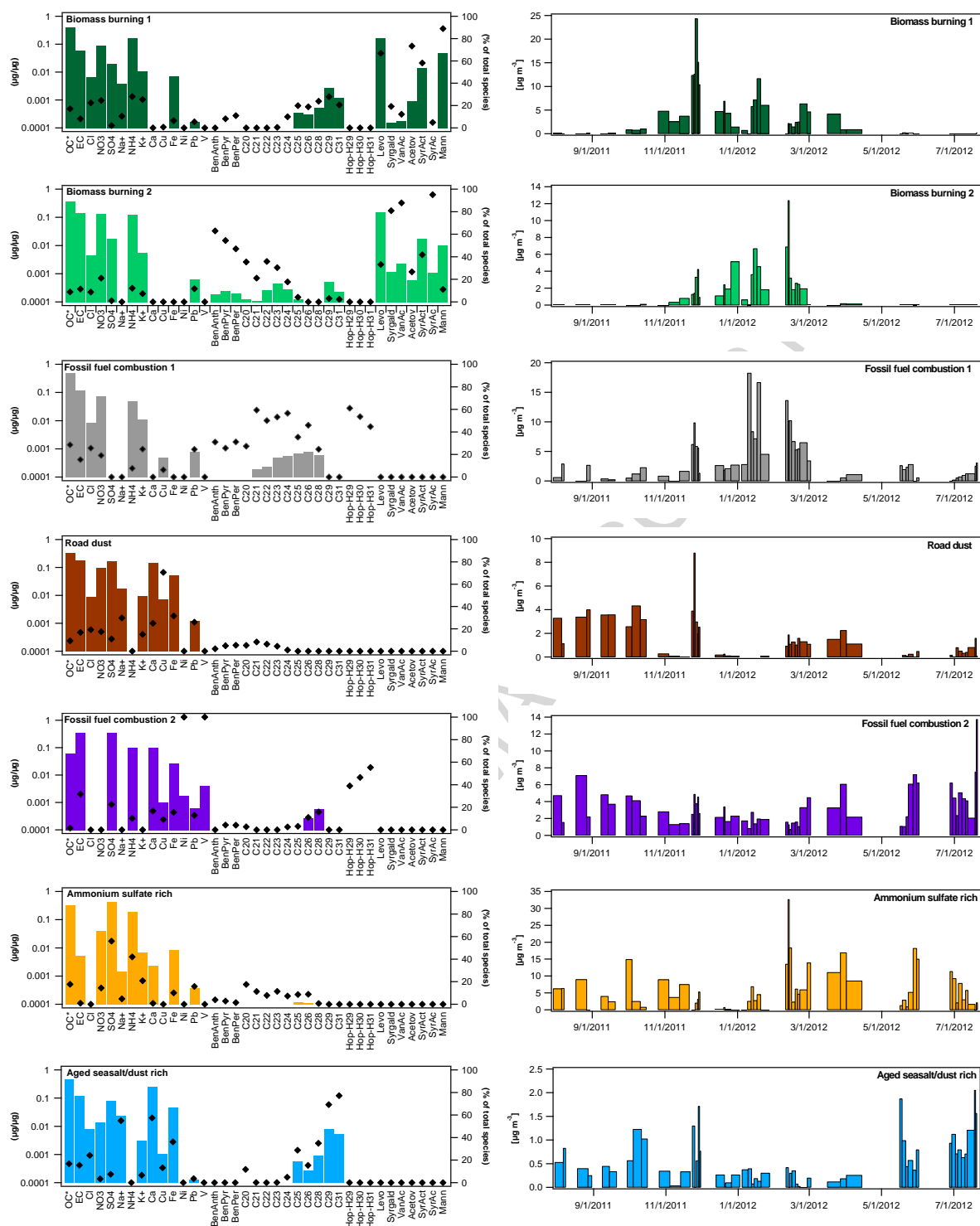


Figure 1: Factor profiles (bars, $\mu\text{g}/\mu\text{g}$, left axis) identified for $\text{PM}_{2.5}$, and percentage of ambient species concentration apportioned by each factor is indicated in the right axis (black diamonds) in the left panels. The time trends of the factor contributions ($\mu\text{g}\cdot\text{m}^{-3}$) is shown in the right panels.

Notes: BenAnth: benzo[a]anthracene; BenPyr: benzo[a]pyrene; BenPer: benzo[ghi]perylene; C20 to C31: *n*-alkanes; Hop-H29: 17 α (H)-21 β (H)-norhopane; Hop-H30: 17 α (H)-21 β (H)-hopane; Hop-H31: 17 α (H)-21 β (H)-22S-homohopane; Levo: levoglucosan; Syrgald: syringaldehyde; VanAc: vanillic acid; Acetov: acetovanillone; SyrAct: syringyl acetone; SyrAc: syringic acid; Mann: mannosan.

3.2. Contributions and seasonality of PM_{2.5} sources

The seasonal mean contributions (in %) of the seven identified sources to the PM_{2.5} mass for the full year (2011-2012) are presented in **Figure 2**, while the seasonal variations of the absolute contributions ($\mu\text{g m}^{-3}$) are reported in **Figure 3**. On an annual basis, the major contributors to the PM_{2.5} mass were the AS-rich and the sum of the biomass burning factors. They accounted for 30% ($6.0 \pm 6.3 \mu\text{g m}^{-3}$) and 23% ($4.5 \pm 6.0 \mu\text{g m}^{-3}$) of the total PM_{2.5} mass, respectively. FF1 and FF2 also contributed significantly to fine aerosol mass with percentage contributions being 19% ($3.6 \pm 4.1 \mu\text{g m}^{-3}$) and 18% ($3.5 \pm 2.3 \mu\text{g m}^{-3}$), respectively, whereas road dust and aged sea salt/dust rich presented far lower concentrations, and accounted only for 7% ($1.4 \pm 1.7 \mu\text{g m}^{-3}$) and 3% ($0.6 \pm 0.5 \mu\text{g m}^{-3}$) of PM_{2.5} mass, respectively. However, the seasonal variations of the seven identified sources reflected a singular pattern for each source which is related to the influence of anthropogenic activities (source strengths), and/or meteorological parameters.

The AS-rich factor showed relatively homogeneous concentrations throughout the year, despite the significant differences in the boundary layer, higher mean contributions were observed during spring ($9.0 \pm 6.8 \mu\text{g m}^{-3}$; 54%) (**Fig. 2, 3**), which indicates an enhanced photochemical production of AS during the warm season owing to the increased oxidation of SO₂ and its conversion rate to sulfate.

As expected, the biomass burning factors (BB1 and BB2) showed a strong seasonality with higher mean concentrations observed in fall and winter (**Fig. 3**). BB1 related to open green waste burning was the dominant contributor to PM_{2.5} mass during fall with an average of 33% ($7.4 \pm 7.6 \mu\text{g m}^{-3}$), while BB2 related to residential heating exhibited the highest contributions during winter ($3.3 \pm 3 \mu\text{g m}^{-3}$; 14%) (**Fig. 2, 3**).

FF1 displayed strong seasonal patterns similar to those of organic markers (hopanes, PAH, and *n*-alkanes; **Fig. A-2**), with significantly higher contributions observed in winter ($7.2 \pm 4.9 \mu\text{g m}^{-3}$; 30%) and fall ($3.0 \pm 3.1 \mu\text{g m}^{-3}$; 13%), compared to spring ($1.4 \pm 1.1 \mu\text{g m}^{-3}$; 8%) and summer ($1.3 \pm 1.1 \mu\text{g m}^{-3}$; 9%) (**Fig. 2, 3**). As mentioned before (**Sect. 3.1**), the higher levels observed in winter can be related to the condensation of semi-volatile organic compounds in the particle phase at low temperature and the stable meteorological conditions in addition to a reduced mixing-layer height favoring the accumulation of pollutants within the emission area.

FF2 exhibited clear seasonal trend with higher contributions recorded in summer ($5.1 \pm 3.0 \mu\text{g m}^{-3}$; 37%) and spring ($4.0 \pm 2.4 \mu\text{g m}^{-3}$; 24%), compared to winter ($2.0 \pm 1.0 \mu\text{g m}^{-3}$; 8%) and fall ($3.2 \pm 1.2 \mu\text{g m}^{-3}$; 14%) (**Fig. 2, 3**). The high levels observed during the hot seasons could be explained by (i) summer wind patterns favoring the transport of industrial and ship emissions from the industrial/harbor area of Fos-Berre located northwest the city (El Haddad et al., 2011a), and (ii) the increased of shipping emissions due to the large number of tourist ships at the harbors during the holiday period (Mazzei et al., 2008).

Road dust showed distinct seasonal pattern with higher levels in fall ($2.9 \pm 2.4 \mu\text{g m}^{-3}$; 13%) and summer ($1.4 \pm 1.4 \mu\text{g m}^{-3}$; 10%), compared to winter ($0.6 \pm 0.7 \mu\text{g m}^{-3}$; 3%) and spring ($0.7 \pm 0.8 \mu\text{g m}^{-3}$; 4%) (**Fig. 2, 3**). These observations seem to be related to pollution episodes that occur during fall and to the resuspension of dust more efficient during the dry period in summer.

The aged sea salt/dust rich factor presented the lowest contribution in winter ($0.2 \pm 0.1 \mu\text{g m}^{-3}$; 1%) and relatively homogeneous and quite higher contributions in the other seasons ($0.6\text{-}0.9 \mu\text{g m}^{-3}$; 3-7%) (Fig. 2, 3), which is probably related to the enhancement of the sea breeze regime accomplished with higher wind intensity velocities.

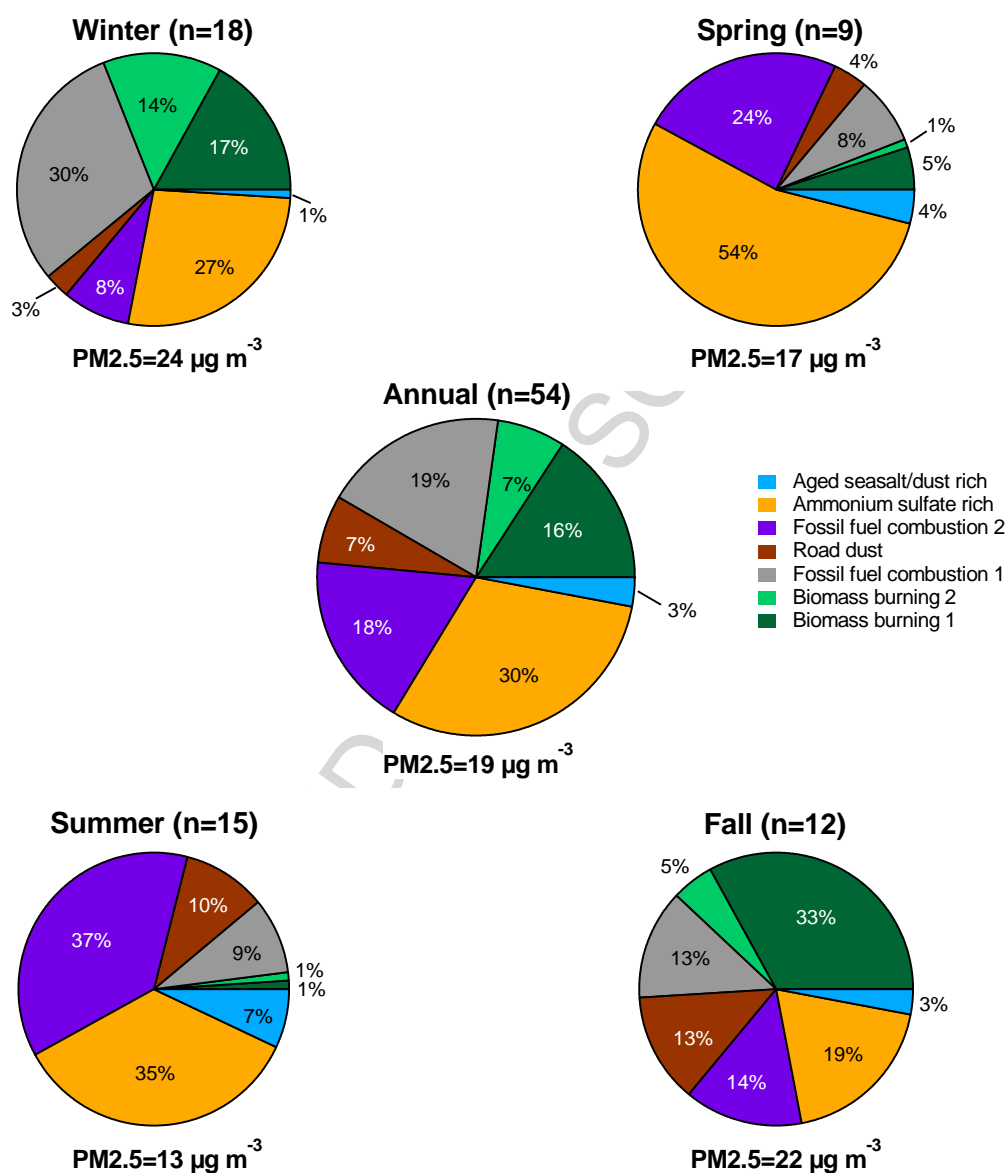


Figure 2 : Annual and seasonal relative mean contributions (in %) of the seven identified factors to the $\text{PM}_{2.5}$ mass. Note that n corresponds to the number of $\text{PM}_{2.5}$ samples.

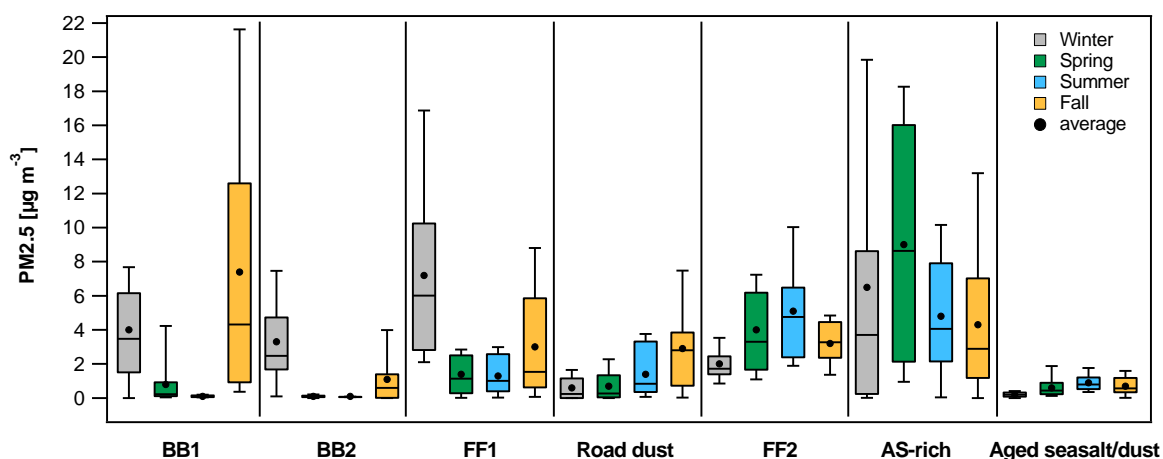


Figure 3 : Seasonal variation of the absolute source contributions ($\mu\text{g m}^{-3}$) to the $\text{PM}_{2.5}$ concentration. Note that the color code denotes the four seasons and the black dot indicates the average seasonal value.

3.3. Insights into PM pollution episodes: potential key sources

This section provides a general overview of the major $\text{PM}_{2.5}$ sources responsible for the pollution episodes ($\text{PM}_{2.5} > 25 \mu\text{g m}^{-3}$) occurring in Marseille during our monitoring period. **Figure 4** displays the contributions of the identified sources ($\mu\text{g m}^{-3}$; %) to $\text{PM}_{2.5}$ mass both during pollution episodes where $\text{PM}_{2.5}$ concentrations were above $25 \mu\text{g m}^{-3}$, and for the periods without such exceedances ($\text{PM}_{2.5} < 25 \mu\text{g m}^{-3}$). We note that the WHO daily limit of $25 \mu\text{g m}^{-3}$ was adopted here because of the lack of a European daily threshold for $\text{PM}_{2.5}$ (WHO, 2006). As displayed in **Figure 4**, total BB appeared to be the first major contributor to $\text{PM}_{2.5}$ mass during pollution episodes ($n=12$ samples and 32 days), and accounted for 33% ($11.9 \pm 7.4 \mu\text{g m}^{-3}$), against 16% ($2.4 \pm 3.4 \mu\text{g m}^{-3}$) for the periods where $\text{PM}_{2.5}$ concentrations were below $25 \mu\text{g m}^{-3}$. Since higher $\text{PM}_{2.5}$ concentrations and pollution episodes are observed in fall and winter (Salameh et al., 2015), this result is not surprising. FF1 displayed a similar behavior, with a substantial contribution during pollution episodes and accounted for 23% ($8.2 \pm 4.4 \mu\text{g m}^{-3}$) of $\text{PM}_{2.5}$ mass, against 15% ($2.3 \pm 3.1 \mu\text{g m}^{-3}$) during the non-exceedance periods (**Fig. 4**). The situation is more complex for the AS-rich factor, because if during pollution episodes, its absolute contribution to $\text{PM}_{2.5}$ mass significantly increases ($10.1 \pm 9.4 \mu\text{g m}^{-3}$ against $4.8 \pm 4.6 \mu\text{g m}^{-3}$), its relative contribution remains rather stable (29% against 32%). This behavior reflects the nature of this fraction that is characteristic of an aged aerosol, relatively homogeneous in terms of concentrations at the regional scale. Conversely, the other sources (i.e. FF2, road dust, and aged sea salt) presented fairly stable concentrations during pollution episodes and the non-exceedance periods, and thus showed lower relative contributions during pollution episodes.

Overall, this analysis reflects to what extent biomass burning and FF1 (likely dominated by traffic emissions) are taking part to $\text{PM}_{2.5}$ critical events, being sources emitted over and/or around the city, thus potentially reduced by the implementation of local and regional actions. However, the relatively high and stable contribution of the AS-rich factor claims for a widespread (national to transnational) effort. Actually, spring and summer pollution episodes were more likely driven by secondary organic

and inorganic formation processes. Thus, mitigation strategies should also be developed for gaseous precursors emissions, in particular NO_x , SO_2 , NH_3 and VOCs at both local and regional scales.

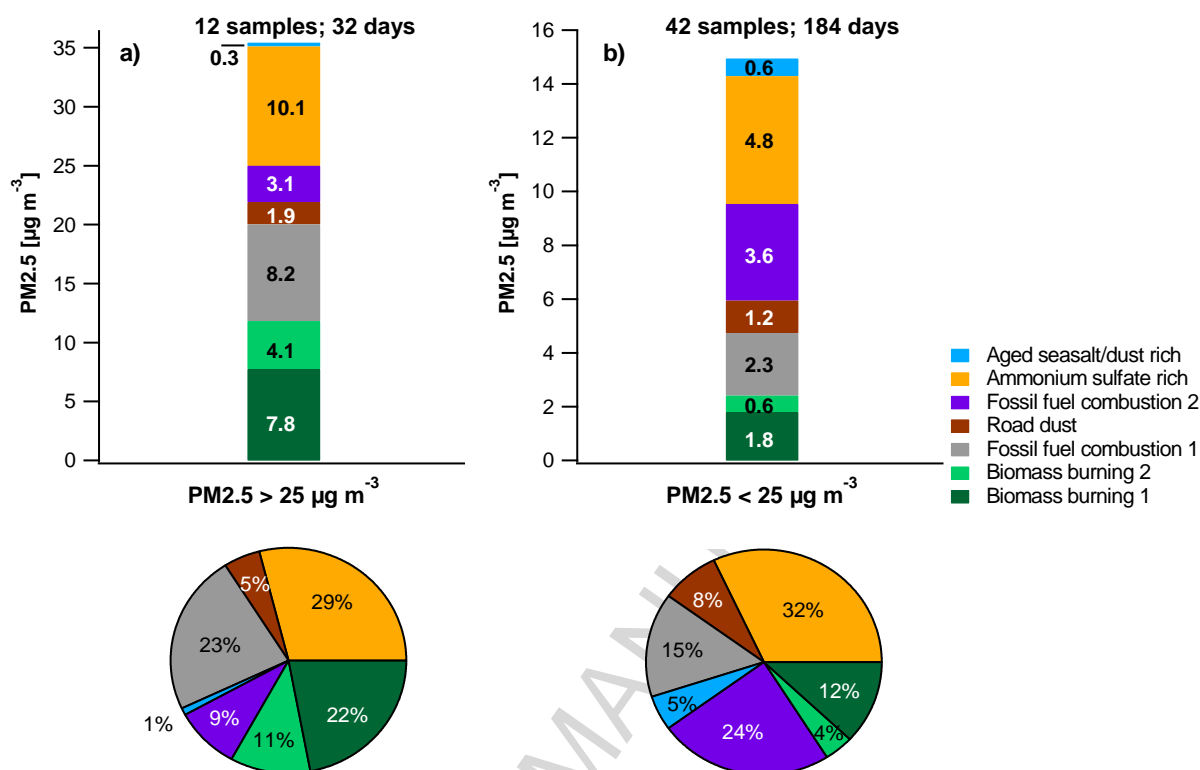


Figure 4: Contributions of the identified sources ($\mu\text{g m}^{-3}$; %) to $\text{PM}_{2.5}$ mass, **(a)** during pollution episodes where $\text{PM}_{2.5}$ concentrations were above $25 \mu\text{g m}^{-3}$ ($\text{PM}_{2.5} > 25 \mu\text{g m}^{-3}$), and **(b)** for the periods without such exceedances ($\text{PM}_{2.5} < 25 \mu\text{g m}^{-3}$).

4. Conclusion

A constrained PMF analysis was applied to a comprehensive $\text{PM}_{2.5}$ dataset (i.e. large array of organic and inorganic tracers) collected over a one-year period (July 2011-July 2012) at an urban background site in Marseille. Constrained PMF results highlighted the relevance of using additional chemical constraints to improve the resolving power of the PMF and to generate cleaner factor profiles and their corresponding contributions.

Two biomass burning factors were resolved and clearly related to different processes, i.e. BB1 related to open green waste burning and BB2 related to residential heating during the coldest periods. Another interesting result was the separation of two fossil fuel combustion processes, the first (FF1) likely dominated by traffic emissions (high contributions of hopanes), and the second (FF2) likely dominated by the harbor/industrial activities (V, Ni, EC). The other identified factors were assigned to ammonium sulfate (AS) rich, road dust, and aged sea salt/dust rich.

On annual average, the major contributors to $\text{PM}_{2.5}$ mass were AS-rich (30%; $6.0 \mu\text{g m}^{-3}$) and the sum of the biomass burning factors (23%; $4.5 \mu\text{g m}^{-3}$). They were followed by FF1 (19%; $3.6 \mu\text{g m}^{-3}$)

³), FF2 (18%; 3.5 $\mu\text{g m}^{-3}$), road dust (7%; 1.4 $\mu\text{g m}^{-3}$), and aged seasalt/dust rich (3%; 0.6 $\mu\text{g m}^{-3}$). AS-rich showed relatively homogeneous absolute contributions throughout the year with high contributions during the warm seasons (35-54%). On the contrary, BB1 showed the highest contribution in fall (33%; 7.4 $\mu\text{g m}^{-3}$) and BB2 in winter (14%; 3.3 $\mu\text{g m}^{-3}$). FF1 contributed the most in winter (30%; 7.2 $\mu\text{g m}^{-3}$), while FF2 presented the highest contribution in summer (37%; 5.1 $\mu\text{g m}^{-3}$). The road dust showed the highest contributions in fall (13%; 2.9 $\mu\text{g m}^{-3}$).

This study revealed that during high PM pollution episodes ($\text{PM}_{2.5} > 25 \mu\text{g m}^{-3}$), the largest contributing sources to $\text{PM}_{2.5}$ were biomass burning (33%) and FF1 (dominated by traffic) (23%). During these episodes, a significant absolute contribution also arises from AS-rich. Therefore, the design of local mitigation actions to tackle $\text{PM}_{2.5}$ concentrations in Marseille should be focused on biomass burning and traffic sources, without disregarding the impacts of meteorological conditions on PM concentration levels. However, a national to transnational plan to abate gaseous precursors (e.g. NO_x , SO_2 , NH_3 and VOCs) from different sources is demanded.

Conflict of interest

The authors declare that they do not have any actual or potential financial and personal conflict of interests with other people or organizations.

Acknowledgments

This work has been supported by the MED program (APICE, grant number 2G-MED09-026: <http://www.apice-project.eu>). PhD Grant: French Environment and Energy Management Agency (ADEME) and Provence Alpes Cote d'Azur (PACA). J. Pey currently benefits from a Ramón y Cajal Research Grant (RYC-2013-14159) from the Spanish Ministry of Economy and Competitiveness. The annual calibration ACTRIS of the OC/EC measurements performed within the APICE project has received funding from the European Union Seventh Framework Programme (FP7/2007-2013) under grant agreement n°262254. Part of the OC/EC analysis carried out in Marseille has been supported by the French national CARA program. This program is directed by O. Favez (INERIS; <http://www.ineris.fr>). He is gratefully acknowledged. The authors gratefully acknowledge the NOAA Air Resources Laboratory (ARL) for providing the HYSPLIT transport and dispersion model and the access to the GDAS meteorological files (<ftp://arlftp.arlhq.noaa.gov/pub/archives/gdas1/>).

References

- Aceves, M., Grimalt, J.O., 1993. Seasonally dependent size distributions of aliphatic and polycyclic aromatic hydrocarbons in urban aerosols from densely populated areas. *Environ. Sci. Technol.* 27, 2896–2908. doi:10.1021/es00049a033
- Agrawal, H., Welch, W.A., Miller, J.W., Cocker, D.R., 2008. Emission Measurements from a Crude Oil Tanker at Sea. *Environ. Sci. Technol.* 42, 7098–7103. doi:10.1021/es703102y
- Almeida, S.M., Lage, J., Fernández, B., Garcia, S., Reis, M.A., Chaves, P.C., 2015. Chemical characterization of atmospheric particles and source apportionment in the vicinity of a steelmaking industry. *Sci. Total Environ.* 521–522, 411–420. doi:10.1016/j.scitotenv.2015.03.112
- Amato, F., Alastuey, A., Karanasiou, A., Lucarelli, F., Nava, S., Calzolari, G., Severi, M., Becagli, S., Gianelle, V.L., Colombi, C., Alves, C., Custódio, D., Nunes, T., Cerqueira, M., Pio, C., Eleftheriadis, K., Diapouli, E., Reche, C., Minguillón, M.C., Manousakas, M.-I., Maggos, T., Vratolis, S., Harrison, R.M., Querol, X., 2016. AIRUSE-LIFE+: a harmonized PM speciation and source apportionment in five southern European cities. *Atmos. Chem. Phys.* 16, 3289–3309. doi:10.5194/acp-16-3289-2016
- Bari, M.A., Baumbach, G., Kuch, B., Scheffknecht, G., 2010. Temporal variation and impact of wood smoke pollution on a residential area in southern Germany. *Atmos. Environ.* 44, 3823–3832. doi:10.1016/j.atmosenv.2010.06.031
- Belis, C.A., Karagulian, F., Larsen, B.R., Hopke, P.K., 2013. Critical review and meta-analysis of ambient particulate matter source apportionment using receptor models in Europe. *Atmos. Environ.* 69, 94–108. doi:http://dx.doi.org/10.1016/j.atmosenv.2012.11.009
- Belis, C. A., Larsen, B., Amato, F., El Haddad, I., Favez, O., Harrison, R. M., Hopke, P. K., Nava, S., Paatero, P., Prévôt, A., Quass, U., Vecchi, R., and Viana, M. 2014. European Guide on Air Pollution Source Apportionment with Receptor Models, p. 88. Publication Office of the European Union, Italy (http://source-apportionment.jrc.ec.europa.eu/Docu/EU_guide_on_SA.pdf).
- Birch, M.E., Cary, R.A., 1996. Elemental Carbon-Based Method for Monitoring Occupational Exposures to Particulate Diesel Exhaust. *Aerosol Sci. Technol.* 25, 221–241. doi:10.1080/02786829608965393
- Bove, M.C., Broto, P., Cassola, F., Cuccia, E., Massabò, D., Mazzino, A., Piazzalunga, A., Prati, P., 2014. An integrated PM_{2.5} source apportionment study: Positive Matrix Factorisation vs. the Chemical Transport Model CAMx. *Atmos. Environ.* doi:10.1016/j.atmosenv.2014.05.039
- Bozzetti, C., Daellenbach, K.R., Hueglin, C., Fermo, P., Sciare, J., Kasper-Giebl, A., Mazar, Y., Abbaszade, G., El Kazzi, M., Gonzalez, R., Shuster-Meiseles, T., Flasch, M., Wolf, R., Křepelová, A., Canonaco, F., Schnelle-Kreis, J., Slowik, J.G., Zimmermann, R., Rudich, Y., Baltensperger, U., El Haddad, I., Prévôt, A.S.H., 2016. Size-Resolved Identification, Characterization, and Quantification of Primary Biological Organic Aerosol at a European Rural Site. *Environ. Sci. Technol.* 50, 3425–3434. doi:10.1021/acs.est.5b05960
- Bozzetti, C., Haddad, I. El, Salameh, D., Daellenbach, K.R., Fermo, P., Gonzalez, R., Minguillón, M.C., Iinuma, Y., Poulain, L., Müller, E., Slowik, J.G., Jaffrezo, J.-L., Baltensperger, U., Marchand, N., Prévôt, A.S.H., 2017a. Organic aerosol source apportionment by offline-AMS over a full year in Marseille. *Atmos. Chem. Phys. Discuss.* 1–46. doi:10.5194/ACP-2017-54
- Bozzetti, C., Sosedova, Y., Xiao, M., Daellenbach, K.R., Ulevicius, V., Dudoitis, V., Mordas, G., Byčenkienė, S., Plauškaitė, K., Vlachou, A., Golly, B., Chazeau, B., Besombes, J.-L., Baltensperger, U., Jaffrezo, J.-L., Slowik, J.G., El Haddad, I., Prévôt, A.S.H., 2017b. Argon offline-AMS source apportionment of organic aerosol over yearly cycles for an urban, rural, and marine site in northern Europe. *Atmos. Chem. Phys.* 17, 117–141. doi:10.5194/acp-17-117-2017
- Callén, M.S., de la Cruz, M.T., López, J.M., Navarro, M. V, Mastral, A.M., 2009. Comparison of receptor models for source apportionment of the PM₁₀ in Zaragoza (Spain). *Chemosphere* 76, 1120–1129. doi:http://dx.doi.org/10.1016/j.chemosphere.2009.04.015
- Callén, M.S., Ilturmendi, A., López, J.M., 2014. Source apportionment of atmospheric PM_{2.5}-bound polycyclic aromatic hydrocarbons by a PMF receptor model. Assessment of potential risk for human health. *Environ. Pollut.* 195, 167–177. doi:10.1016/j.envpol.2014.08.025

- Canonaco, F., Crippa, M., Slowik, J.G., Baltensperger, U., Prévôt, A.S.H., 2013. SoFi, an IGOR-based interface for the efficient use of the generalized multilinear engine (ME-2) for the source apportionment: ME-2 application to aerosol mass spectrometer data. *Atmos. Meas. Tech.* 6, 3649–3661. doi:10.5194/amt-6-3649-2013
- Cavalli, F., Viana, M., Yttri, K.E., Genberg, J., Putaud, J.P., 2010. Toward a standardised thermal-optical protocol for measuring atmospheric organic and elemental carbon: the EUSAAR protocol. *Atmos. Meas. Tech.* 3, 79–89. doi:10.5194/amt-3-79-2010
- Cesari, D., Donato, A., Conte, M., Merico, E., Giangreco, A., Giangreco, F., Contini, D., 2016. An inter-comparison of PM_{2.5} at urban and urban background sites: Chemical characterization and source apportionment. *Atmos. Res.* 174, 106–119. doi:10.1016/j.atmosres.2016.02.004
- Cusack, M., Pérez, N., Pey, J., Alastuey, A., Querol, X., 2013. Source apportionment of fine PM and sub-micron particle number concentrations at a regional background site in the western Mediterranean: a 2.5 year study. *Atmos. Chem. Phys.* 13, 5173–5187. doi:10.5194/acp-13-5173-2013
- Daellenbach, K.R., Bozzetti, C., Křepelová, A., Canonaco, F., Wolf, R., Zotter, P., Fermo, P., Crippa, M., Slowik, J.G., Sosedova, Y., Zhang, Y., Huang, R.-J., Poulain, L., Szidat, S., Baltensperger, U., El Haddad, I., Prévôt, A.S.H., 2016. Characterization and source apportionment of organic aerosol using offline aerosol mass spectrometry. *Atmos. Meas. Tech.* 9, 23–39. doi:10.5194/amt-9-23-2016
- Dockery, D.W., 2009. Health effects of particulate air pollution. *Ann Epidemiol* 19, 257–263. doi:10.1016/j.annepidem.2009.01.018
- Dutton, S.J., Vedal, S., Piedrahita, R., Milford, J.B., Miller, S.L., Hannigan, M.P., 2010. Source apportionment using positive matrix factorization on daily measurements of inorganic and organic speciated PM_{2.5}. *Atmos. Environ.* 44, 2731–2741. doi:http://dx.doi.org/10.1016/j.atmosenv.2010.04.038
- El Haddad, I., D'Anna, B., Temime-Roussel, B., Nicolas, M., Boreave, A., Favez, O., Voisin, D., Sciare, J., George, C., Jaffrezo, J.L., Wortham, H., Marchand, N., 2013. Towards a better understanding of the origins, chemical composition and aging of oxygenated organic aerosols: case study of a Mediterranean industrialized environment, Marseille. *Atmos. Chem. Phys.* 13, 7875–7894. doi:10.5194/acp-13-7875-2013
- El Haddad, I., Marchand, N., Dron, J., Temime-Roussel, B., Quivet, E., Wortham, H., Jaffrezo, J.L., Baduel, C., Voisin, D., Besombes, J.L., Gille, G., 2009. Comprehensive primary particulate organic characterization of vehicular exhaust emissions in France. *Atmos. Environ.* 43, 6190–6198. doi:http://dx.doi.org/10.1016/j.atmosenv.2009.09.001
- El Haddad, I., Marchand, N., Wortham, H., Piot, C., Besombes, J.-L., Cozic, J., Chauvel, C., Armengaud, A., Robin, D., Jaffrezo, J.-L., 2011a. Primary sources of PM_{2.5} organic aerosol in an industrial Mediterranean city, Marseille. *Atmos. Chem. Phys.* 11, 2039–2058. doi:10.5194/acp-11-2039-2011
- El Haddad, I., Marchand, N., Wortham, H., Temime-Roussel, B., Piot, C., Besombes, J.-L., Baduel, C., Voisin, D., Armengaud, A., Jaffrezo, J.-L., 2011b. Insights into the secondary fraction of the organic aerosol in a Mediterranean urban area: Marseille. *Atmos. Chem. Phys.* 11, 2059–2079. doi:10.5194/acp-11-2059-2011
- Flaounas, E., Coll, I., Armengaud, A., Schmechtig, C., 2009. The representation of dust transport and missing urban sources as major issues for the simulation of PM episodes in a Mediterranean area. *Atmos. Chem. Phys.* 9, 8091–8101. doi:10.5194/acp-9-8091-2009
- Graham, B., Guyon, P., Taylor, P.E., Artaxo, P., Maenhaut, W., Glovsky, M.M., Flagan, R.C., Andreae, M.O., 2003. Organic compounds present in the natural Amazonian aerosol: Characterization by gas chromatography–mass spectrometry. *J. Geophys. Res. Atmos.* 108, 4766. doi:10.1029/2003JD003990
- Grythe, H., Ström, J., Krejci, R., Quinn, P., Stohl, A., 2014. A review of sea-spray aerosol source functions using a large global set of sea salt aerosol concentration measurements. *Atmos. Chem. Phys.* 14, 1277–1297. doi:10.5194/acp-14-1277-2014
- Hans Wedepohl, K., 1995. The composition of the continental crust. *Geochim. Cosmochim. Acta* 59, 1217–1232. doi:http://dx.doi.org/10.1016/0016-7037(95)00038-2
- Hays, M.D., Geron, C.D., Linna, K.J., Smith, N.D., Schauer, J.J., 2002. Speciation of Gas-Phase and Fine Particle Emissions from Burning of Foliar Fuels. *Environ. Sci. Technol.* 36, 2281–2295. doi:10.1021/es0111683

Hedberg, E., Johansson, C., Johansson, L., Swietlicki, E., Brorström-Lundén, E., 2006. Is Levoglucosan a Suitable Quantitative Tracer for Wood Burning? Comparison with Receptor Modeling on Trace Elements in Lycksele, Sweden. *J. Air Waste Manage. Assoc.* 56, 1669–1678. doi:10.1080/10473289.2006.10464572

Heo, J., Dulger, M., Olson, M.R., McGinnis, J.E., Shelton, B.R., Matsunaga, A., Sioutas, C., Schauer, J.J., 2013. Source apportionments of PM_{2.5} organic carbon using molecular marker Positive Matrix Factorization and comparison of results from different receptor models. *Atmos. Environ.* 73, 51–61. doi:10.1016/j.atmosenv.2013.03.004

Hopke, P.K., 2010. The Application of Receptor Modeling to Air Quality Data. *Pollut. atmos* 91–109.

Huang, R.-J., Zhang, Y., Bozzetti, C., Ho, K.-F., Cao, J.-J., Han, Y., Daellenbach, K.R., Slowik, J.G., Platt, S.M., Canonaco, F., Zotter, P., Wolf, R., Pieber, S.M., Bruns, E.A., Crippa, M., Ciarelli, G., Piazzalunga, A., Schwikowski, M., Abbaszade, G., Schnelle-Kreis, J., Zimmermann, R., An, Z., Szidat, S., Baltensperger, U., El Haddad, I., Prévôt, A.S.H., 2014. High secondary aerosol contribution to particulate pollution during haze events in China. *Nature* 514, 218–222. doi:10.1038/nature13774

Hwang, I., Hopke, P.K., 2007. Estimation of source apportionment and potential source locations of PM_{2.5} at a west coastal IMPROVE site. *Atmos. Environ.* 41, 506–518. doi:10.1016/j.atmosenv.2006.08.043

Hwang, I., Hopke, P.K., 2006. Comparison of Source Apportionments of Fine Particulate Matter at Two San Jose Speciation Trends Network Sites. *J. Air Waste Manage. Assoc.* 56, 1287–1300. doi:10.1080/10473289.2006.10464586

Jaekels, J.M., Bae, M.-S., Schauer, J.J., 2007. Positive Matrix Factorization (PMF) Analysis of Molecular Marker Measurements to Quantify the Sources of Organic Aerosols. *Environ. Sci. Technol.* 41, 5763–5769. doi:10.1021/es062536b

Jaffrezo, J.L., Aymoz, G., Cozic, J., 2005. Size distribution of EC and OC in the aerosol of Alpine valleys during summer and winter. *Atmos. Chem. Phys.* 5, 2915–2925. doi:10.5194/acp-5-2915-2005

Jaffrezo, J.L., Calas, N., Bouchet, M., 1998. Carboxylic acids measurements with ionic chromatography. *Atmos. Environ.* 32, 2705–2708. doi:http://dx.doi.org/10.1016/S1352-2310(98)00026-0

Jedynska, A., Hoek, G., Eeftens, M., Cyrus, J., Keuken, M., Ampe, C., Beelen, R., Cesaroni, G., Forastiere, F., Cirach, M., de Hoogh, K., De Nazelle, A., Madsen, C., Declercq, C., Eriksen, K.T., Katsouyanni, K., Akhlaghi, H.M., Lanki, T., Meliefste, K., Nieuwenhuijsen, M., Oldenwening, M., Pennanen, A., Raaschou-Nielsen, O., Brunekreef, B., Kooter, I.M., 2014. Spatial variations of PAH, hopanes/steranes and EC/OC concentrations within and between European study areas. *Atmos. Environ.* 87, 239–248. doi:10.1016/j.atmosenv.2014.01.026

Jedynska, A., Hoek, G., Wang, M., Eeftens, M., Cyrus, J., Beelen, R., Cirach, M., De Nazelle, A., Keuken, M., Visschedijk, A., Nystad, W., Akhlaghi, H.M., Meliefste, K., Nieuwenhuijsen, M., de Hoogh, K., Brunekreef, B., Kooter, I.M., 2015. Spatial variations of levoglucosan in four European study areas. *Sci. Total Environ.* 505, 1072–1081. doi:10.1016/j.scitotenv.2014.10.091

Karanasiou, A.A., Siskos, P.A., Eleftheriadis, K., 2009. Assessment of source apportionment by Positive Matrix Factorization analysis on fine and coarse urban aerosol size fractions. *Atmos. Environ.* 43, 3385–3395. doi:10.1016/j.atmosenv.2009.03.051

Laden, F., Neas, L.M., Dockery, D.W., Schwartz, J., 2000. Association of fine particulate matter from different sources with daily mortality in six U.S. cities. *Environ. Health Perspect.* 108, 941–7.

Lee, E., Chan, C.K., Paatero, P., 1999. Application of positive matrix factorization in source apportionment of particulate pollutants in Hong Kong. *Atmos. Environ.* 33, 3201–3212. doi:http://dx.doi.org/10.1016/S1352-2310(99)00113-2

Mazzei, F., D'Alessandro, A., Lucarelli, F., Nava, S., Prati, P., Valli, G., Vecchi, R., 2008. Characterization of particulate matter sources in an urban environment. *Sci. Total Environ.* 401, 81–89. doi:http://dx.doi.org/10.1016/j.scitotenv.2008.03.008

Minguillón, M.C., Querol, X., Baltensperger, U., Prévôt, A.S.H., 2012a. Fine and coarse PM composition and sources in rural and urban sites in Switzerland: Local or regional pollution? *Sci. Total Environ.* 427–428, 191–202. doi:http://dx.doi.org/10.1016/j.scitotenv.2012.04.030

Minguillón, M.C., Schembari, A., Triguero-Mas, M., de Nazelle, A., Dadvand, P., Figueras, F., Salvado, J.A., Grimalt, J.O., Nieuwenhuijsen, M., Querol, X., 2012b. Source apportionment of indoor, outdoor and personal PM_{2.5} exposure of pregnant women in Barcelona, Spain. *Atmos. Environ.* 59, 426–436. doi:<http://dx.doi.org/10.1016/j.atmosenv.2012.04.052>

Mooibroek, D., Schaap, M., Weijers, E.P., Hoogerbrugge, R., 2011. Source apportionment and spatial variability of PM_{2.5} using measurements at five sites in the Netherlands. *Atmos. Environ.* 45, 4180–4191. doi:<http://dx.doi.org/10.1016/j.atmosenv.2011.05.017>

Moreno, T., Querol, X., Alastuey, A., de la Rosa, J., Sánchez de la Campa, A.M., Minguillón, M., Pandolfi, M., González-Castanedo, Y., Monfort, E., Gibbons, W., 2010. Variations in vanadium, nickel and lanthanoid element concentrations in urban air. *Sci. Total Environ.* 408, 4569–4579. doi:<http://dx.doi.org/10.1016/j.scitotenv.2010.06.016>

Norris, G.A., Duvall, R., 2014. EPA Positive Matrix Factorization (PMF) 5.0 Fundamentals and User guide

Norris, G., Vedantham, R., Wade, K., Zhan, P., Brown, S., Pentti, P., Eberly, S., and Foley, C., 2009. Guidance Document for PMF Applications with the Multilinear Engine. U.S. Environ. Prot. Agency, Washington, DC, EPA/600/R-09/032 (NTIS PB2009-107895).

Oros, D.R., Simoneit, B.R.T., 2000. Identification and emission rates of molecular tracers in coal smoke particulate matter. *Fuel* 79, 515–536. doi:[http://dx.doi.org/10.1016/S0016-2361\(99\)00153-2](http://dx.doi.org/10.1016/S0016-2361(99)00153-2)

Paatero, P. 2004. User's Guide for Positive Matrix Factorization Programs PMF2 and PMF3. Part. 1: Tutorial. University of Helsinki, Department of Physics, Finland

Paatero, P., 1999. The Multilinear Engine—A Table-Driven, Least Squares Program for Solving Multilinear Problems, Including the n-Way Parallel Factor Analysis Model. *J. Comput. Graph. Stat.* 8, 854–888. doi:[10.1080/10618600.1999.10474853](http://dx.doi.org/10.1080/10618600.1999.10474853)

Paatero, P., 1997. Least squares formulation of robust non-negative factor analysis. *Chemom. Intell. Lab. Syst.* 37, 23–35. doi:[10.1016/s0169-7439\(96\)00044-5](http://dx.doi.org/10.1016/s0169-7439(96)00044-5)

Paatero, P., Hopke, P.K., 2009. Rotational tools for factor analytic models. *J. Chemom.* 23, 91–100. doi:[10.1002/cem.1197](http://dx.doi.org/10.1002/cem.1197)

Paatero, P., Hopke, P.K., 2003. Discarding or downweighting high-noise variables in factor analytic models. *Anal. Chim. Acta* 490, 277–289. doi:[10.1016/s0003-2670\(02\)01643-4](http://dx.doi.org/10.1016/s0003-2670(02)01643-4)

Paatero, P., Hopke, P.K., Begum, B.A., Biswas, S.K., 2005. A graphical diagnostic method for assessing the rotation in factor analytical models of atmospheric pollution. *Atmos. Environ.* 39, 193–201. doi:<http://dx.doi.org/10.1016/j.atmosenv.2004.08.018>

Paatero, P., Hopke, P.K., Song, X.H., Ramadan, Z., 2002. Understanding and controlling rotations in factor analytic models. *Chemom. Intell. Lab. Syst.* 60, 253–264. doi:[10.1016/s0169-7439\(01\)00200-3](http://dx.doi.org/10.1016/s0169-7439(01)00200-3)

Paatero, P., Tapper, U., 1994. Positive matrix factorization: A non-negative factor model with optimal utilization of error estimates of data values. *Environmetrics* 5, 111–126. doi:[10.1002/env.3170050203](http://dx.doi.org/10.1002/env.3170050203)

Pandolfi, M., Gonzalez-Castanedo, Y., Alastuey, A., Rosa, J., Mantilla, E., Campa, A.S., Querol, X., Pey, J., Amato, F., Moreno, T., 2011. Source apportionment of PM₁₀ and PM_{2.5} at multiple sites in the strait of Gibraltar by PMF: impact of shipping emissions. *Environ. Sci. Pollut. Res.* 18, 260–269. doi:[10.1007/s11356-010-0373-4](http://dx.doi.org/10.1007/s11356-010-0373-4)

Pérez, N., Pey, J., Querol, X., Alastuey, A., López, J.M., Viana, M., 2008. Partitioning of major and trace components in PM₁₀–PM_{2.5}–PM₁ at an urban site in Southern Europe. *Atmos. Environ.* 42, 1677–1691. doi:[10.1016/j.atmosenv.2007.11.034](http://dx.doi.org/10.1016/j.atmosenv.2007.11.034)

Pey, J., Alastuey, A., Querol, X., 2013a. PM₁₀ and PM_{2.5} sources at an insular location in the western Mediterranean by using source apportionment techniques. *Sci. Total Environ.* 456–457, 267–77. doi:[10.1016/j.scitotenv.2013.03.084](http://dx.doi.org/10.1016/j.scitotenv.2013.03.084)

Pey, J., Pérez, N., Cortés, J., Alastuey, A., Querol, X., 2013b. Chemical fingerprint and impact of shipping emissions over a western Mediterranean metropolis: Primary and aged contributions. *Sci. Total Environ.* 463–464, 497–507. doi:<http://dx.doi.org/10.1016/j.scitotenv.2013.06.061>

- Pio, C.A., Castro, L.M., Cerqueira, M.A., Santos, I.M., Belchior, F., Salgueiro, M.L., 1996. Source assessment of particulate air pollutants measured at the southwest european coast. *Atmos. Environ.* 30, 3309–3320. doi:10.1016/1352-2310(96)00058-1
- Polissar, A. V., Hopke, P.K., Poirot, R.L., 2001. Atmospheric Aerosol over Vermont: Chemical Composition and Sources. *Environ. Sci. Technol.* 35, 4604–4621. doi:10.1021/es0105865
- Pope, C.A., Dockery, D.W., 2006. Health effects of fine particulate air pollution: lines that connect. *J. Air Waste Manag. Assoc.* 56, 709–42.
- Putaud, J.P., Van Dingenen, R., Alastuey, A., Bauer, H., Birmili, W., Cyrys, J., Flentje, H., Fuzzi, S., Gehrig, R., Hansson, H.C., Harrison, R.M., Herrmann, H., Hitzenberger, R., Hüglin, C., Jones, A.M., Kasper-Giebl, A., Kiss, G., Kousa, A., Kuhlbusch, T.A.J., Löschau, G., Maenhaut, W., Molnar, A., Moreno, T., Pekkanen, J., Perrino, C., Pitz, M., Puxbaum, H., Querol, X., Rodriguez, S., Salma, I., Schwarz, J., Smolik, J., Schneider, J., Spindler, G., ten Brink, H., Tursic, J., Viana, M., Wiedensohler, A., Raes, F., 2010. A European aerosol phenomenology – 3: Physical and chemical characteristics of particulate matter from 60 rural, urban, and kerbside sites across Europe. *Atmos. Environ.* 44, 1308–1320. doi:http://dx.doi.org/10.1016/j.atmosenv.2009.12.011
- Puxbaum, H., Caseiro, A., Sánchez-Ochoa, A., Kasper-Giebl, A., Claeys, M., Gelencsér, A., Legrand, M., Preunkert, S., Pio, C., 2007. Levoglucosan levels at background sites in Europe for assessing the impact of biomass combustion on the European aerosol background. *J. Geophys. Res. Atmos.* 112, D23S05. doi:10.1029/2006JD008114
- Reche, C., Viana, M., Amato, F., Alastuey, A., Moreno, T., Hillamo, R., Teinilä, K., Saarnio, K., Seco, R., Peñuelas, J., Mohr, C., Prévôt, A.S.H., Querol, X., 2012. Biomass burning contributions to urban aerosols in a coastal Mediterranean City. *Sci. Total Environ.* 427–428, 175–190. doi:http://dx.doi.org/10.1016/j.scitotenv.2012.04.012
- Rogge, W.F., Hildemann, L.M., Mazurek, M.A., Cass, G.R., Simoneit, B.R.T., 1993. Sources of fine organic aerosol. 4. Particulate abrasion products from leaf surfaces of urban plants. *Environ. Sci. Technol.* 27, 2700–2711. doi:10.1021/es00049a008
- Salameh, D., Detournay, A., Pey, J., Pérez, N., Liguori, F., Saraga, D., Bove, M.C., Broto, P., Cassola, F., Massabò, D., Latella, A., Pillon, S., Formenton, G., Patti, S., Armengaud, A., Piga, D., Jaffrezo, J.L., Bartzis, J., Tolis, E., Prati, P., Querol, X., Wortham, H., Marchand, N., 2015. PM_{2.5} chemical composition in five European Mediterranean cities: a one-year study. *Atmos. Res.* 155, 102–117. doi:10.1016/j.atmosres.2014.12.001
- Schauer, J.J., Lough, G.C., Shafer, M.M., Christensen, W.F., Arndt, M.F., DeMinter, J.T., Park, J.-S., 2006. Characterization of metals emitted from motor vehicles. *Res. Rep. Health. Eff. Inst.* 1-76-88.
- Schembari, C., Bove, M.C., Cuccia, E., Cavalli, F., Hjorth, J., Massabò, D., Nava, S., Udisti, R., Prati, P., 2014. Source apportionment of PM₁₀ in the Western Mediterranean based on observations from a cruise ship. *Atmos. Environ.* 98, 510–518. doi:10.1016/j.atmosenv.2014.09.015
- Seinfeld, J.H., Pandis, S.N., 1998. Atmospheric chemistry and physics: From air pollution to climate change. John Wiley & Sons, New York. doi:10.1063/1.882420
- Shrivastava, M.K., Subramanian, R., Rogge, W.F., Robinson, A.L., 2007. Sources of organic aerosol: Positive matrix factorization of molecular marker data and comparison of results from different source apportionment models. *Atmos. Environ.* 41, 9353–9369. doi:http://dx.doi.org/10.1016/j.atmosenv.2007.09.016
- Simoneit, B.R.T., Schauer, J.J., Nolte, C.G., Oros, D.R., Elias, V.O., Fraser, M.P., Rogge, W.F., Cass, G.R., 1999. Levoglucosan, a tracer for cellulose in biomass burning and atmospheric particles. *Atmos. Environ.* 33, 173–182. doi:http://dx.doi.org/10.1016/S1352-2310(98)00145-9
- Simoneit, B.R.T., Sheng, G., Chen, X., Fu, J., Zhang, J., Xu, Y., 1991. Molecular marker study of extractable organic matter in aerosols from urban areas of China. *Atmos. Environ. Part A. Gen. Top.* 25, 2111–2129. doi:10.1016/0960-1686(91)90088-O
- Sternbeck, J., Sjödin, Å., Andréasson, K., 2002. Metal emissions from road traffic and the influence of resuspension—results from two tunnel studies. *Atmos. Environ.* 36, 4735–4744. doi:http://dx.doi.org/10.1016/S1352-2310(02)00561-7

Sylvestre, A., Mizzi, A., Mathiot, S., Masson, F., Jaffrezo, J.L., Dron, J., Mesbah, B., Wortham, H., Marchand, N., 2017. Comprehensive chemical characterization of industrial PM_{2.5} from steel industry activities. *Atmos. Environ.* 152, 180–190. doi:10.1016/j.atmosenv.2016.12.032

Taiwo, A.M., Beddows, D.C.S., Calzolari, G., Harrison, R.M., Lucarelli, F., Nava, S., Shi, Z., Valli, G., Vecchi, R., 2014. Receptor modelling of airborne particulate matter in the vicinity of a major steelworks site. *Sci. Total Environ.* 490, 488–500. doi:http://dx.doi.org/10.1016/j.scitotenv.2014.04.118

Tolis, E., Saraga, D., Ammari, G., Gkanas, E., Gougoulas, T., Papaioannou, C., Sarioglou, A., Kougioumtzidis, E., Skemperi, A., Bartzis, J., 2014. Chemical characterization of particulate matter (PM) and source apportionment study during winter and summer period for the city of Kozani, Greece. *Cent. Eur. J. Chem.* 12, 643–651. doi:10.2478/s11532-014-0531-5

Vecchi, R., Chiari, M., D'Alessandro, A., Fermo, P., Lucarelli, F., Mazzei, F., Nava, S., Piazzalunga, A., Prati, P., Silvani, F., Valli, G., 2008. A mass closure and PMF source apportionment study on the sub-micron sized aerosol fraction at urban sites in Italy. *Atmos. Environ.* 42, 2240–2253. doi:http://dx.doi.org/10.1016/j.atmosenv.2007.11.039

Viana, M., Amato, F., Alastuey, A., Querol, X., Moreno, T., Dos Santos, S.G., Herce, M.D., Fernandez-Patier, R., 2009. Chemical tracers of particulate emissions from commercial shipping. *Env. Sci Technol* 43, 7472–7477.

Viana, M., Hammingh, P., Colette, A., Querol, X., Degraeuwe, B., Vlieger, I. de, van Aardenne, J., 2014. Impact of maritime transport emissions on coastal air quality in Europe. *Atmos. Environ.* 90, 96–105. doi:10.1016/j.atmosenv.2014.03.046

Viana, M., Kuhlbusch, T.A.J., Querol, X., Alastuey, A., Harrison, R.M., Hopke, P.K., Winiwarter, W., Vallius, M., Szidat, S., Prévôt, A.S.H., Hueglin, C., Bloemen, H., Wählin, P., Vecchi, R., Miranda, A.I., Kasper-Giebl, A., Maenhaut, W., Hitenberger, R., 2008. Source apportionment of particulate matter in Europe: A review of methods and results. *J. Aerosol Sci.* 39, 827–849. doi:http://dx.doi.org/10.1016/j.jaerosci.2008.05.007

Vossler, T., Černíkovský, L., Novák, J., Williams, R., 2016. Source apportionment with uncertainty estimates of fine particulate matter in Ostrava, Czech Republic using Positive Matrix Factorization. *Atmos. Pollut. Res.* doi:10.1016/j.apr.2015.12.004

Waked, A., Favez, O., Alleman, L.Y., Piot, C., Petit, J.E., Delaunay, T., Verlinden, E., Golly, B., Besombes, J.L., Jaffrezo, J.L., Leoz-Garziandia, E., 2014. Source apportionment of PM₁₀ in a north-western Europe regional urban background site (Lens, France) using positive matrix factorization and including primary biogenic emissions. *Atmos. Chem. Phys.* 14, 3325–3346. doi:10.5194/acp-14-3325-2014

Watson, J.G., Antony Chen, L.-W., Chow, J.C., Doraiswamy, P., Lowenthal, D.H., 2008. Source Apportionment: Findings from the U.S. Supersites Program. *J. Air Waste Manage. Assoc.* 58, 265–288. doi:10.3155/1047-3289.58.2.265

Watson, J.G., Chow, J.C., Lu, Z., Fujita, E.M., Lowenthal, D.H., Lawson, D.R., Ashbaugh, L.L., 1994. Chemical Mass Balance Source Apportionment of PM₁₀ during the Southern California Air Quality Study. *Aerosol Sci. Technol.* 21, 1–36. doi:10.1080/02786829408959693

Watson, J.G., Robinson, N.F., Chow, J.C., Henry, R.C., Kim, B.M., Pace, T.G., Meyer, E.L., Nguyen, Q., 1990. The USEPA/DRI chemical mass balance receptor model, CMB 7.0. *Environ. Softw.* 5, 38–49. doi:10.1016/0266-9838(90)90015-X

Weitkamp, E.A., Lipsky, E.M., Pancras, P.J., Ondov, J.M., Polidori, A., Turpin, B.J., Robinson, A.L., 2005. Fine particle emission profile for a large coke production facility based on highly time-resolved fence line measurements. *Atmos. Environ.* 39, 6719–6733. doi:http://dx.doi.org/10.1016/j.atmosenv.2005.06.028

WHO, 2006. Air quality guidelines. Global update 2005. Particulate matter, ozone, nitrogen dioxide and sulfur dioxide. World Health Organization, Regional Office for Europe, Copenhagen, Denmark (http://whqlibdoc.who.int/hq/2006/WHO_SDE_PHE_OEH_06.02_eng.pdf).

Zhang, Y., Schauer, J.J., Zhang, Y., Zeng, L., Wei, Y., Liu, Y., Shao, M., 2008. Characteristics of Particulate Carbon Emissions from Real-World Chinese Coal Combustion. *Environ. Sci. Technol.* 42, 5068–5073. doi:10.1021/es7022576

Zhang, Y., Sheesley, R.J., Schauer, J.J., Lewandowski, M., Jaoui, M., Offenberg, J.H., Kleindienst, T.E., Edney, E.O., 2009. Source apportionment of primary and secondary organic aerosols using positive matrix factorization (PMF) of molecular markers. *Atmos. Environ.* 43, 5567–5574. doi:10.1016/j.atmosenv.2009.02.047

ACCEPTED MANUSCRIPT

Highlights:

- A constrained PMF analysis (ME2) successfully applied with a large array of organic and inorganic markers
- Two distinct fingerprints for biomass burning resolved
- Two signatures for the fossil fuel combustion processes separated
- Secondary processes and biomass burning emissions are the major contributors to PM_{2.5}

ACCEPTED MANUSCRIPT